water

MDPI

Article

Numerical Simulation of the External Water Pressure in Seepage Anisotropy Under Heterogeneous Conditions

Jixian Shen [1], Hongbin Ma [2], Hengheng Du [3], Yawen Xin [3,*], Haining Liu [3] and Wenjia Ma [3]

[1] Northern Henan Water Conservancy Project Management Bureau, Xinxiang 453002, China; ybjggk@126.com
[2] Henan Shuitou Xiaolangdi North Bank Irrigation District Engineering Co., Ltd., Zhengzhou 450003, China; z202210020237@stu.ncwu.edu.cn
[3] College of Geosciences and Engineering, North China University of Water Resources and Electric Power, Zhengzhou 450046, China; z202210020267@stu.ncwu.edu.cn (H.D.); lhngeo@yahoo.com.cn (H.L.); b202200217@stu.ncwu.edu.cn (W.M.)
* Correspondence: yawenxin@hhu.edu.cn

Abstract: The external water pressure and seepage quantity are crucial factors in tunnel construction design, especially under complex geological conditions. Both analytical solutions and numerical simulations can be used to calculate the external water pressure in a shallow circular cross-section tunnel. Analytical formulas are usually derived based on homogeneous surrounding rock, which seems somehow unrealistic. In reality, the engineering geological conditions are complex and the surrounding rock is heterogeneous. Therefore, the results of analytical formulas may deviate from the actual results. This study takes the No. 1 shallow-buried tunnel in the north bank of the Xiaolangdi irrigation area as its research background. Based on heterogeneous and anisotropic analyses, the horizontal permeability, the vertical permeability, the parameters of the lining and grouting circle, and the position head are the main factors affecting the stability of the external water pressure. The result shows that the external water pressure increases as the ratio of the horizontal permeability coefficient to the vertical permeability coefficient increases. Moreover, when a grouting ring is used to block the water, the lining is guaranteed to have a certain degree of permeability, which helps to better achieve the purpose of reducing the external water pressure.

Keywords: complicated geological; heterogeneity; anisotropy; external water pressure of lining; numerical simulation

Citation: Shen, J.; Ma, H.; Du, H.; Xin, Y.; Liu, H.; Ma, W. Numerical Simulation of the External Water Pressure in Seepage Anisotropy Under Heterogeneous Conditions. *Water* **2024**, *16*, 3173. https://doi.org/10.3390/w16223173

Academic Editor: Giuseppe Pezzinga

Received: 10 October 2024
Revised: 25 October 2024
Accepted: 4 November 2024
Published: 6 November 2024

1. Introduction

An increasing number of tunnel engineering projects have emerged since the concept of deep subterranean construction was implemented. The implementation of these projects promotes the development of underground space, but also brings many technical challenges. Among them, groundwater leakage is regarded as a major risk factor, and its potential consequences include the collapse of the tunnel structure, hazards to workers' lives, and delayed progress on the project [1,2]. In addition, excessive groundwater discharge not only affects the construction process, but also may lead to serious environmental problems, or even cause irreversible damage to the ecosystem [3,4]. Under complex groundwater conditions, accurately calculating the tunnel's external water pressure has become a practical problem that cannot be ignored in tunnel construction and operation. Usually, when assessing the various factors affecting external water pressure, we typically take into account the geological environment of the tunnel, the permeability characteristics of the surrounding rock, the permeability of the lining itself, and the impacts of drainage and grouting measures [5–7].

Currently, there are two main methods for the analysis and treatment of external water pressure. One is analytical calculation, and the other is numerical calculation. Early scholars derived an analytical formula for predicting seepage in tunnels using the circular tunnel model [8–10]. Subsequent scholars refined this analytical formula and broadened its application scope, proposing an analytical method that addresses the steady-state seepage field within tunnels, influenced by the action of the grouting circle [11,12].

Subsequently, scholars have carried out more in-depth research and proposed an analytical solution to determine the seepage pressure in non-circular tunnels based on a circular tunnel model. Duan et al. [13] proposed an exact axisymmetric analytical solution for the seepage flow and external water pressure values of the surrounding rock, lining, and grouting ring under high outside water pressure. This offers a new theoretical solution to use when researching the water pressure value of non-circular hydraulic tunnels. Zhao et al. [14] examined the water pressure and reduction coefficient of a horseshoe section tunnel lining, and their findings were corroborated by engineering examples. They also provided recommended values for the thickness of the grouting ring and its external water pressure reduction coefficient, pertaining to the grouting effect. Yu et al. [15], Liu et al. [16], and Bi et al. [17] derived an analytical solution that applies to a tunnel seepage field with a drainage system. With the continuous advancement and refinement of computer technology, the application of numerical methods in engineering and scientific research has significantly escalated. In the past few decades, researchers have developed a variety of software programs based on the finite element method (FEM) and the discrete element method (DEM). These tools are used for in-depth analyses of steady and transient conditions of groundwater flow [18,19].

Arjnoi P et al. [20] used ABAQUS to simulate a drainage circular tunnel under steady groundwater flow conditions and studied the influence of pore water pressure distribution on lining stress. Zhang et al. [21] used ABAQUS software to develop a three-dimensional numerical calculation program, taking the Xianglushan diversion tunnel in the water diversion project in central Yunnan as the research background. The program aims to deeply analyze the influence of lining parameters, grouting layer parameters, and drainage holes on the seepage pressure of the surrounding rock and linings under different working conditions. Yu et al. [22] and Li et al. [23] used numerical simulations to study the influence of different waterproof drainage parameters on seepage fields. Lv et al. [24] used MODFLOW software to evaluate the influence of tunnel excavation on groundwater flow.

To summarize, modern studies on tunnels mainly focus on controlling the infiltration of tunnels and the external pressure of water. Investigations primarily focus on drainage tactics, the grouting ring's thickness and permeability coefficient, and the lining's thickness and permeability coefficient, aiming to modify the tunnel seepage field in different conditions. However, the lack of an understanding of the actual geological conditions of the surrounding rock that describe external water pressure in the analytical solution poses a significant challenge, primarily due to the complexities of tunnel boundary conditions and anisotropy. These software packages can not only simulate complex groundwater flows, but also evaluate the influence of different parameters on the flow characteristics so as to provide a scientific basis for decision-making. This paper addresses this gap by utilizing a numerical simulation for analyzing external water pressure, with a particular focus on the heterogeneous surrounding rock and anisotropic permeability. Many of these solutions are predicated on assumptions that are more applicable to deeply buried tunnels, rendering them less accurate for shallow tunnels. Numerical simulation was employed to address complex problems with a high degree of precision. To accomplish the task of tunnel waterproofing and drainage, an investigation of the parameters of the composite lining is crucial. Finally, we studied the influence of a composite lining's material parameters on external water pressure under the conditions of heterogeneous geological conditions and seepage anisotropy.

2. Research Background and Geological Conditions

2.1. Project Profile

The Xiaolangdi north irrigation area project is located on the north bank of the Yellow River in Henan Province. It is a large (2) type irrigation area. The No. 1 tunnel in the section of pile No. ZG19 + 090 ~ ZG21 + 030 in the research is a part of the hilly bedrock region. The ground elevation is generally 218~249 m. The tunnel′s subterranean depth is between 16 and 22 m, and the groundwater level is 2.8~20 m higher than the tunnel floor. There are drainage problems in the construction of underground tunnels, which increases the risk of a tunnel water inrush. The location of the study area is shown in Figure 1.

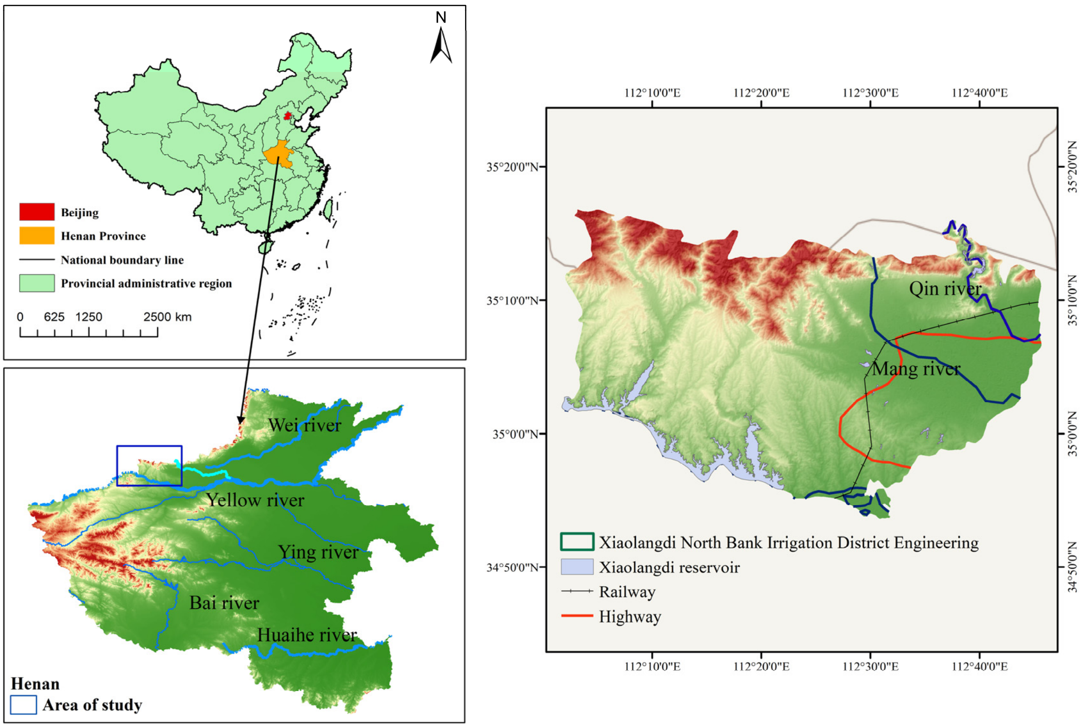

Figure 1. Location of the study area.

2.2. Geological Conditions

In order to identify the properties and classifications of the surrounding rocks of the tunnel, an additional borehole, designated as SW20 + 265A, was drilled to a depth of 30 m. Figure 2 shows the strata distribution. Various mechanical and hydrogeological tests were conducted to obtain the geomechanical properties of the No. 1 tunnel site. In addition, a substantial number of permeability tests were conducted within the boreholes throughout the tunnel to determine the permeability of each layer.

Level	Depth /m	Thickness /m	Drilling columnar structure	Soil type
1	0.00			
2	8.20	8.20		Heavy silt loam
3	14.00	5.80		Mudstone
4	16.70	2.70		Sandstone
5	21.10	4.50		Mudstone
6	30.00	8.90		Sandstone

Figure 2. Strata distribution of the test borehole.

The surrounding rock lithology of the No. 1 tunnel section is mainly Paleogene strata. The engineering geological classification of the Paleogene surrounding rock is V class, and the engineering geological classification of the loess surrounding rock is V class. The underground water level in this section is high, predominantly situated near the interface of soil and rock, and the loess in this area exhibits medium permeability, while the bedrock displays weak permeability. Moreover, this borehole showed that the geological structure type belongs to a soil–rock bilayer structure. The strata that were drilled can be divided into five layers. The uppermost stratum of the rock formation is composed of heavy silty loam. The remaining four layers exhibit alternating strata of sandstone and mudstone. Among them, the bedrock above the top of the tunnel near pile number ZG19 + 489~ZG19 + 580 is thin. Overlying a 16–20 m thick soil layer, the terrain is low-lying, with upper stagnant water. Also, the integrity of the sandstone rock mass at the top of the cave is poor; there are well-developed cracks, and it would be easy for a seepage channel to form. Affected by high groundwater, the surrounding rock may fall and collapse, and there is a problem of cavern stability. The underground water level in the rock stratum is high, the rock mass is weakly permeable, and there is a problem of construction dewatering and drainage.

3. Calculation of Seepage

3.1. Analytical Solution

Here we propose a circular, homogeneous, isotropic tunnel, as shown schematically in Figure 3, with the following assumptions: The tunnel is thought to be in a steady state, and the surrounding rock, lining, and grouting ring are homogeneous and continuous isotropic media of different materials. The groundwater flow follows Darcy's law [25,26]. Furthermore,

r_0—the outer radius of the tunnel,
r_m—the outer radius of the secondary lining,
r_c—the outer radius of the primary support,
r_g—the outer radius of the grouting ring,
r_s—the outer radius of the surrounding rock,
H—the outer head of the tunnel,
H_m—the outer water head of the lining,
H_c—the outer water head of the support,
H_g—the outer water head of the grouting ring,
K_s—the permeability coefficient of the surrounding rock,
K_g—the permeability coefficient of the grouting ring,
K_c—the permeability coefficient of the primary support,
K_m—the permeability coefficient of the secondary lining.

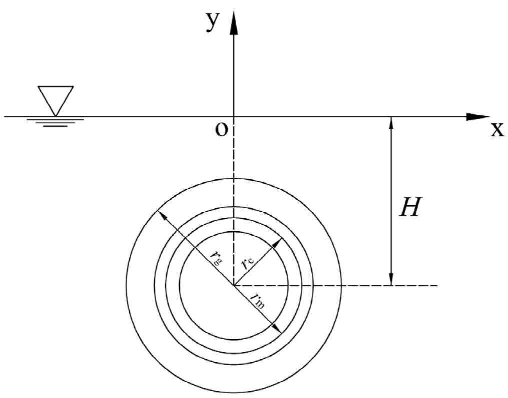

Figure 3. Tunnel simplified model.

To satisfy the seepage continuity equation (Laplace Equation):

$$\nabla^2 H = 0 \tag{1}$$

$$\frac{1}{r}\frac{\partial}{\partial r}\left(r\frac{\partial H}{\partial r}\right)+\frac{1}{r^2}\frac{\partial^2 H}{\partial \theta^2}+\frac{\partial^2 H}{\partial z^2}=0 \tag{2}$$

The Z axis and the water flow are perpendicular, so $\frac{\partial H}{\partial Z}=0$. At the same time, about the tunnel axis Z, the head field function H exhibits symmetry, thus $\frac{\partial H}{\partial \theta}=0$. One way to simplify Formula (2) is as follows:

$$\frac{1}{r}\frac{\mathrm{d}}{\mathrm{d}r}\left(r\frac{\mathrm{d}H}{\mathrm{d}r}\right)=0 \tag{3}$$

Furthermore, $r \neq 0$, thus

$$r\frac{\mathrm{d}H}{\mathrm{d}r}=\mathrm{C} \tag{4}$$

Based on the above modeling analysis, an analytical formula for the calculation of tunnel seepage can be derived under specific assumptions.

(1) Analytical formula for the seepage volume in the Harr Tunnel

Utilizing the mirror method, Harr [5] reimagined the semi-infinite seepage field of a tunnel as the superposition of two infinite seepage fields. This was predicated on the assumption that the initial water table is horizontal and remains constant, the groundwater is in a steady state and conforms to a radial flow, and the medium is homogeneous and isotropic. Consequently, the following analytical formula for calculating the seepage quantity was derived:

$$Q=\frac{2\pi HK}{\ln\left[1+(2H/\mathrm{r}_0)^2\right]^{0.5}} \tag{5}$$

(2) Analytical formula for seepage flow in the Goodman Tunnel

Goodman [6] simplified Harr′s formula using the condition $H >> r$ to obtain the seepage calculation for the tunnel. Goodman's formula is suitable for the calculation of water inflow in high head or deep buried tunnels under runoff conditions.

$$Q=\frac{2\pi H\mathrm{K}}{\ln(2H/\mathrm{r})} \tag{6}$$

(3) Analytical formula for seepage flow in the Ying Hongwei Tunnel

Ying Hongwei [8] developed an analytical formula to describe the seepage field of deeply buried underwater tunnels that include grout rings and liners, utilizing the mirror method. This formula is suitable for conditions with a constant groundwater level, as well as for both deeply and shallowly buried lined tunnels within homogeneous isotropic aquifers.

$$Q=\frac{2\pi K_{\mathrm{s}}H}{\ln\frac{2h_{\mathrm{c}}}{r_{\mathrm{g}}}+\frac{K_{\mathrm{s}}}{K_{\mathrm{g}}}\ln\frac{r_{\mathrm{g}}}{r_{\mathrm{m}}}+\frac{K_{\mathrm{s}}}{K_{\mathrm{m}}}\ln\frac{r_1}{r_0}} \tag{7}$$

3.2. Numerical Calculation Method

The tunnel seepage field is numerically simulated using Midas. With the tunnel in its center, the computational model has dimensions of 60 m × 40 m × 30 m, r_{m} = 2.16 m, r_{c} = 2.36 m, and r_{g} = 2.86 m, respectively. There is a water table 20 m above the bottom of the tunnel in this segment, which is submerged at a depth of 22 m. The model-related material parameters are shown in Table 1.

Table 1. Model-related material parameters.

Material	E/GPa	$K/(m \cdot s^{-1})$	μ
Heavy silt loam	5.6	1.2×10^{-5}	0.4
Mudstone	11.0	1×10^{-7}	0.32
Sandstone	15.0	1×10^{-6}	0.25
Grouting ring	20.0	2×10^{-7}	0.3
Secondary lining	26.5	1.5×10^{-9}	0.2

Note: E—Elastic modulus, K—Permeability coefficient, μ—Poisson′s ratio.

Figure 4 shows a simplified model for the calculation of the seepage field of a submerged tunnel, taking into account the grouting ring, initial support, and secondary lining, with the following assumptions:

(1) The tunnel has a circular cross-section.
(2) The water table line is the upper border. The water pressure at the left and right boundaries is set according to the gradient of the groundwater depth change. Also, the model′s bottom is set to an impermeable border. Drainage is accomplished through consistent seepage through the lining.
(3) The soils are all continuous, anisotropic media, the soils and water are incompressible, and there is adequate groundwater recharge in the seepage field.
(4) The amount of tunnel drainage does not affect the groundwater level, i.e., there is a fixed distance between the center of the tunnel and the line that represents the groundwater level.
(5) Isotropic homogeneous continuous media are used for the grout rings, initial support, and secondary lining.
(6) The seepage obeys Darcy′s law and the tunnel is in a steady state of seepage.

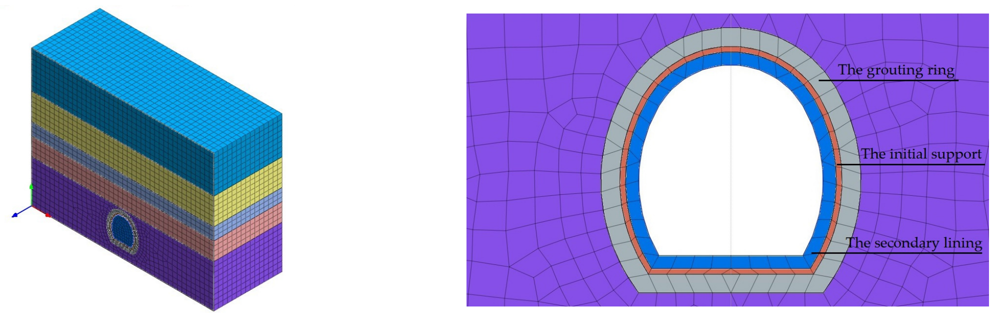

(**a**) Model diagrams with finite element method (**b**) Model of tunnel lining structures

Figure 4. Computational model for numerical simulation.

The horizontal permeability coefficient of the soil around the borehole is K_x. The vertical permeability coefficient is K_y. Permeability runs in the same directions as the main coordinate axes, and the coefficients are all constants. The datum is set on the bottom surface.

3.3. Comparison of Analytical and Numerical Calculations

According to the section design, the permeability coefficients are as follows: $K_s = 1 \times 10^{-6}$ m/s, $K_g = 5 \times 10^{-8}$ m/s, $K_c = 5 \times 10^{-9}$ m/s, and $K_m = 1 \times 10^{-9}$ m/s. The H terms are 9 m, 12 m, 15 m, 17 m, 19 m, and 20 m, respectively. A comparison between the results of each analytical calculation and the numerical solution at various depths of the tunnel is presented in Figure 5.

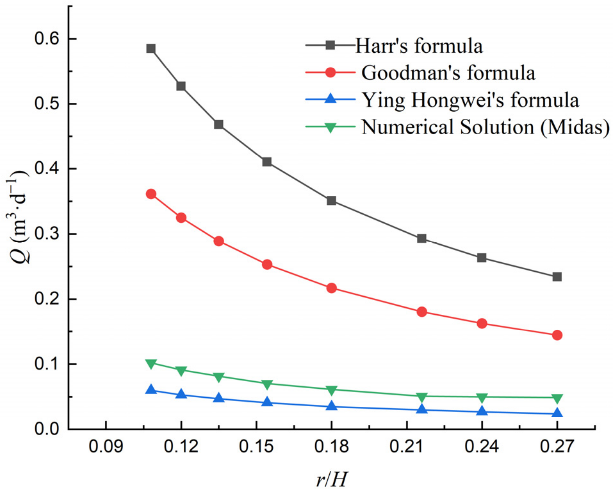

Figure 5. Comparison between analytical solutions and numerical simulations.

Upon analyzing the calculation results, it becomes evident that as the horizontal coordinate r/H increases, the H experiences a gradual decline. Concurrently, the seepage volume, as determined by both the analytical formula and numerical calculation, also diminishes progressively. In terms of comparison, Harr′s formula yields the highest values, whereas Ying′s formula results in the lowest. Notably, the numerical outcomes fall within the range defined by the Goodman and Ying formulas.

This is because Ying′s formula accounts for the water-blocking effect of the grouting ring, which results in a relatively small calculated seepage volume. Furthermore, Harr′s and Goodman′s formulas are typically applicable to high head or deeply buried tunnels, where the overall water head of the tunnel seepage field tends to be greater, leading to a higher calculated seepage volume. The results calculated using these formulas for the seepage quantity of tunnels in shallow-buried tunnels or fractured media are often on the higher result. Generally, these analytical formulas effectively solve the problem of calculating the groundwater inflow into a tunnel, based on the assumption that the surrounding rock constitutes a homogeneous and isotropic seepage environment within a deeply embedded tunnel. However, for tunnels situated in complex geological settings, where the surrounding rock is heterogeneous and the tunnel is shallowly buried, the calculated outcomes can markedly diverge from the real data. In contrast, the numerical calculation method takes into account the impact of a heterogeneous and anisotropic seepage field, yielding results that are more aligned with reality.

4. Discussion

4.1. Analytical Formulas

Estimating the external water pressure in anisotropic seepage scenarios involves considering factors like the horizontal and vertical permeability coefficients, as well as the permeability and thickness of the grouting/lining [27,28].

Under the anisotropic seepage scenario, the external water pressure can be calculated by means of Equations (8) and (9):

$$H_m = \frac{H\left[\frac{K_e}{K_m}\ln(r_m/r_0)\right] + h_0\left[\frac{K_e}{K_g}\ln(r/r_c)\right] + \frac{K_e}{K_c}\ln(r_c/r_m) - \ln\alpha}{\left[\frac{K_e}{K_g}\ln(r/r_c) + \frac{K_e}{K_c}\ln(r_c/r_m) + \frac{K_e}{K_m}\ln(r_m/r_0)\right] - \ln\alpha} \quad (8)$$

$$\beta = \frac{H_m}{H} \quad (9)$$

H_m—External water pressure.

β—Reduction coefficient.

4.2. Calculation Results Analysis

Make the following assumptions: $K_m = 1 \times 10^{-9}$ m/s, $K_c = 5 \times 10^{-9}$ m/s, $K_g = 5 \times 10^{-8}$ m/s, the permeability coefficient of the perimeter rock level takes the value of $K_x = 1 \times 10^{-5}$ m/s, and the vertical permeability coefficient takes the value of $K_y = 1 \times 10^{-6}$ m/s. Taking H values of 10 m, 12 m, 14 m, 16 m, 18 m, and 20 m, Figure 6 shows the numerical computation cloud diagram. Numerical simulations of the seepage quantity and water pressure under various tunnel head height circumstances are compared in Figure 7.

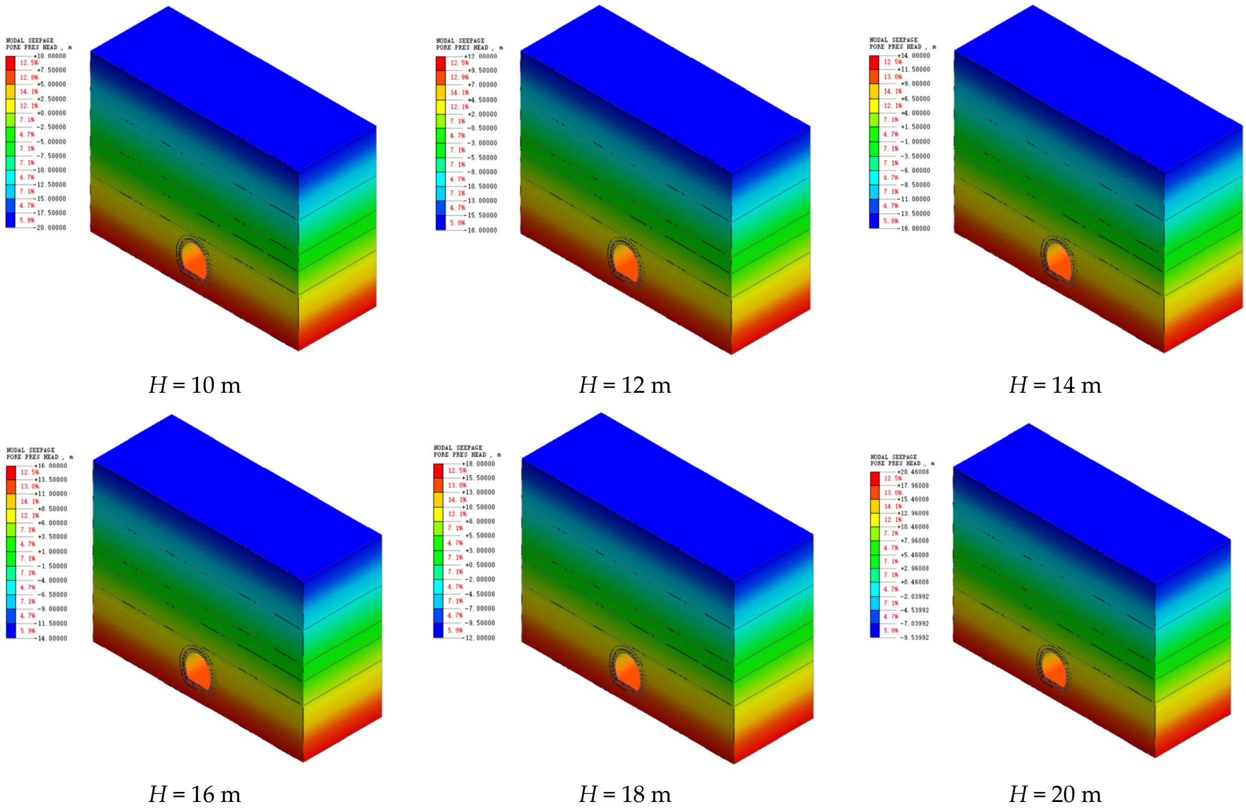

Figure 6. Numerical calculation results for different H values.

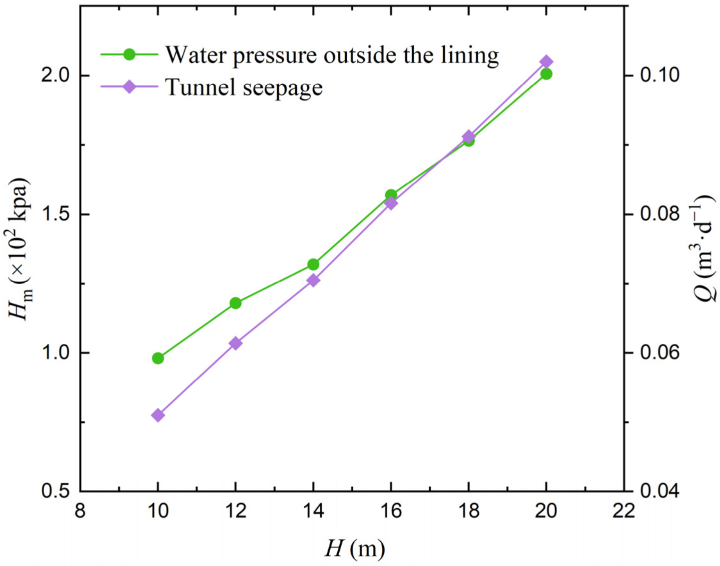

Figure 7. Seepage quantity and water pressure with H.

Figure 6 illustrates how the seepage quantity and external water pressure increase linearly with underground head height. In general, seepage volume rises uniformly with changes in H; the H_m increases first rapidly and then slowly as the head changes. The H_m increases at a rate of 20% when $H < 14$ m. When $H > 14$ m, the H_m increases at a rate of 12%. Overall, the trends in H_m and Q are consistent with each other.

5. Parametric Analysis

5.1. Horizontal and Vertical Permeability Coefficient of Surrounding Rock

To account for the impact of percolation anisotropy, the vertical permeability coefficients of the soil body K_y are set to 1×10^{-6} m/s, 2×10^{-6} m/s, 3×10^{-6} m/s, 4×10^{-6} m/s, 5×10^{-6} m/s, and 6×10^{-6} m/s. The horizontal permeability coefficients K_x are set to 1×10^{-6} m/s, 2×10^{-6} m/s, 5×10^{-5} m/s, 1×10^{-4} m/s, and 2×10^{-4} m/s. The variation curves of the permeability coefficient of the surrounding rock and the water pressure outside the lining are displayed in Figure 8.

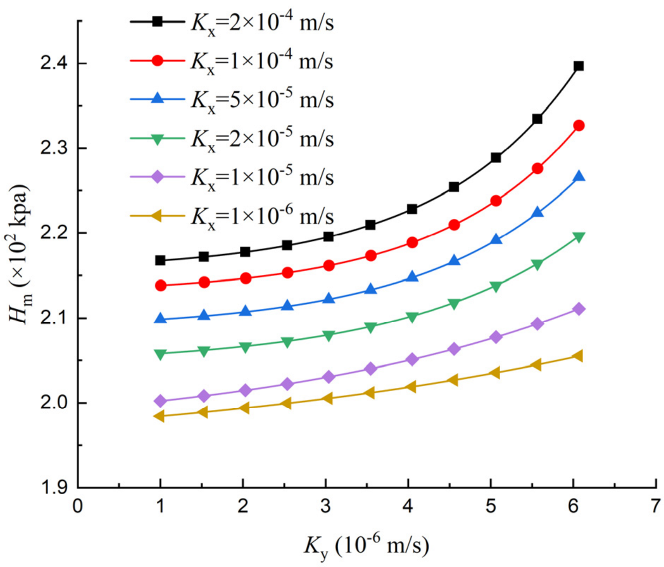

Figure 8. K_x and K_y's influence on H_m.

Increases in the K_x or K_y can enhance the H_m, provided that the material properties of the composite lining remain unchanged. When $K_x = 2 \times 10^{-4}$ m/s, $K_y = 1 \times 10^{-6}$ m/s and $H_m = 2.16 \times 10^2$ kpa. When $K_x = 5 \times 10^{-5}$ m/s, $K_y = 2 \times 10^{-6}$ m/s and $H_m = 2.14 \times 10^2$ kpa. All in all, a correlation exists between K_x and K_y. This correlation has an effect on H_m, which is due to the fact that the surrounding rock is anisotropic.

To better explain the impact of percolation anisotropy, let $n = K_x/K_y$. The magnitude of the ratio n, which represents the relationship between the horizontal transverse permeability coefficient K_x and the vertical permeability coefficient K_y of the soil, can quantify the extent of variation in seepage properties across different directions in the surrounding rock. A higher value of n indicates a more pronounced seepage anisotropy. Suppose the soil's horizontal transverse permeability coefficient, K_x, is a variable with a value of 1×10^{-6} m/s. Let n take on values of 1, 5, 10, 20, 50, 80, 100, and 200. The corresponding variation curves of the permeability coefficient of the surrounding rock and the water pressure outside the lining are depicted in Figure 9.

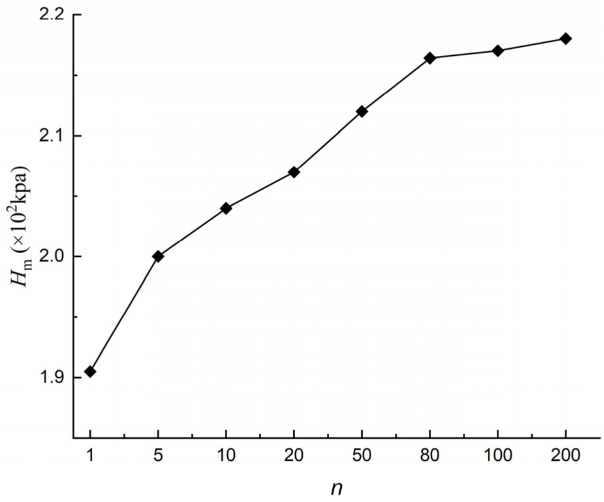

Figure 9. Change in the H_m under different values of n.

As can be seen in Figure 9, a correlation exists between n and H_m, due to the fact that the surrounding rock is anisotropic. The increase in the n value will enhance the H_m, provided that the material properties of the composite lining remain unchanged. Furthermore, when K_x equals 1×10^{-6} m/s and K_y is also 1×10^{-6} m/s (i.e., $n = 1$, indicating seepage anisotropy), the H_m is 1.9×10^2 kpa. In comparison, when $n = 10$, H_m increases to 2.04×10^2 kpa, representing a 7% rise; and when $n = 50$, H_m reaches 2.12×10^2 kpa, a 12% increase. This illustrates that neglecting seepage anisotropy can lead to an underestimation of the water pressure acting on the lining.

5.2. Grout Ring′s Parameters

Let n = 1, 20, 50, 80, and 100, and let t_g represent the grouting circle thicknesses of 0.5 m, 0.6 m, 0.7 m, 0.8 m, 0.9 m, and 1 m. K_g is 5×10^{-6} m/s, 5×10^{-7} m/s, 5×10^{-8} m/s, 5×10^{-9} m/s, and 5×10^{-10} m/s. The relationship between the external water pressure and grout ring parameters is depicted in Figure 10.

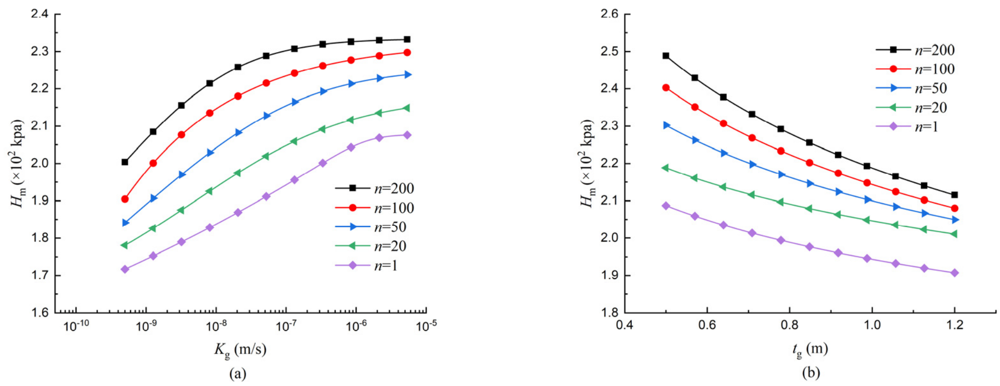

Figure 10. Relationship between H_m and grout ring parameters.

As shown in Figure 10, under steady conditions, with the increase of t_g, H_m first decreases rapidly, which produces an impressive water-blocking effect, then changes to a consistent decline, with the pace of reduction slowly decelerating. The H_m rises with an increase in n when the grouting circle′s thickness remains constant. When $n = 1$, the surrounding rock is seepage isotropic, and the value of H_m is at its lowest. In addition, when $t_g > 0.9$ m and $K_g > 5 \times 10^{-6}$ m/s, when the parameters are modified, the variation in H_m is relatively unremarkable. It can be found that increasing the thickness of the grouting ring has a positive effect of reducing the external water pressure of the lining, but blindly increasing the thickness of the grouting ring is also unreasonable. Oddly, a rise in K_g leads to a significant increase in H_m, followed by a gradual deceleration in the growth rate. Obviously, reducing the K_g has a significant beneficial effect on the H_m, so reducing the permeability coefficient of the grouting ring is an effective construction method to control the external water pressure in the project. In summary, the effectiveness of controlling the H_m in the tunnel does not simply require increasing the grouting ring's thickness or reducing the grouting ring's permeability. Instead, there is an optimal parameter value that is relatively economical and reasonable.

5.3. Lining Parameters

In order to consider the influence of lining parameters on external water pressure, first, let the lining thickness be represented by the values t_m = 0.35 m, 0.45 m, 0.55 m, 0.65 m, 0.75 m, and 0.85 m. It is assumed that the values of K_m are 1×10^{-6} m/s, 1×10^{-7} m/s, 1×10^{-8} m/s, 1×10^{-9} m/s, and 1×10^{-10} m/s. The relationship between the external water pressure and the lining parameters is calculated in Figure 11.

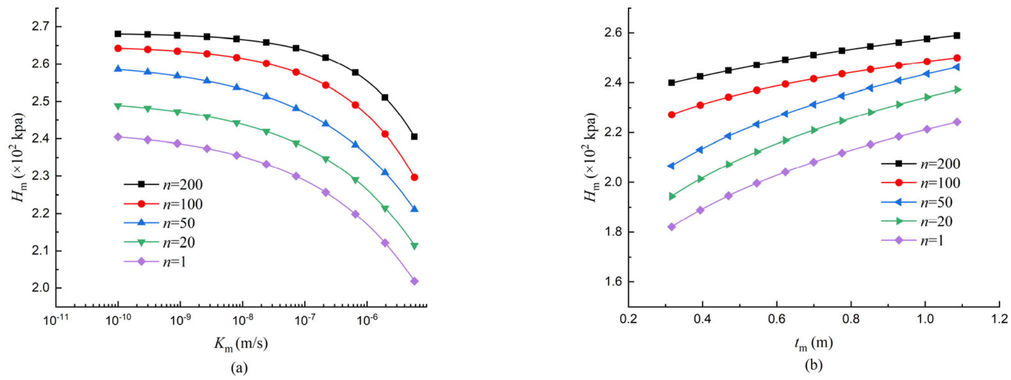

Figure 11. Relationship between H_m and lining parameters.

By observing the graph, we can observe that t_m and K_m have the highest impact on the H_m of the tunnel, and the H_m is also enhanced by permeability anisotropy, which is directly attributable to the n. It should be noted that one of the main factors in the analysis is that when the $K_m > 1 \times 10^{-8}$ m/s, the H_m decreases and the rate of reduction gradually speeds up. When the $K_m < 1 \times 10^{-8}$ m/s, the H_m increases, and the growth rate gradually changes and becomes steady. As the permeability coefficient of the lining increases, the external water pressure decreases. This is because with the increase of the lining's permeability coefficient, groundwater enters the tunnel through the lining, resulting in an increased water inflow. This leads to the dissipation of pore water pressure and a decrease in the lining water pressure.

Second, it is noteworthy to mention that due to the change of t_m, the H_m will also change. The detailed information is as follows. From the trend of the overall change, the bigger the value of n, the less sensitive H_m is to thickness. The impact of the t_m on the H_m is governed by the n value. From Figure 10, it can also be seen that the greater the thickness, the lower the permeability coefficient and the smaller the impact of external water pressure, because the larger the thickness, the smaller the permeability coefficient. The lining blocks all underground water outside the lining, the pore pressure cannot dissipate, and the external water pressure is almost equal to the hydrostatic pressure. Therefore, the value of the thickness should balance drainage and pressure relief with environmental protection. If the lining thickness is too small, it will increase the amount of seepage and damage the environment. If the lining thickness is too large, it will increase the external water pressure, which is not conducive to the stability of the lining, and will also increase the project's cost. In general, to maintain the tunnel's structural integrity, the lining requires a specific thickness. Finally, enhancing the t_m while increasing K_m serves as an efficient strategy to lower the H_m, thereby preserving the tunnel structure's safety and carrying out the drainage operation.

5.4. Relationship Between Tunnel Lining Drainage and External Water Pressure Reduction Factor

In order to consider the relationship between tunnel lining drainage and the external water pressure, it is necessary to consider the relationship between tunnel rise drainage and the external water pressure discount factor. Changes of drainage are achieved by changing the permeability coefficient of the lining.

The equivalent permeability coefficient of the surrounding rock $K_e = 1 \times 10^{-5}$ m/s, the ratio of horizontal to vertical permeability coefficient n is 20, the thickness of the t_g is 0.5 m, and the ratios of the equivalent permeability coefficient of the surrounding rock to the permeability coefficient of the grouting ring are 1, 10, 50, 100, 200, and 500. The relationship between the lining drainage volume and the reduction coefficient of the external water pressure is shown in Figure 12.

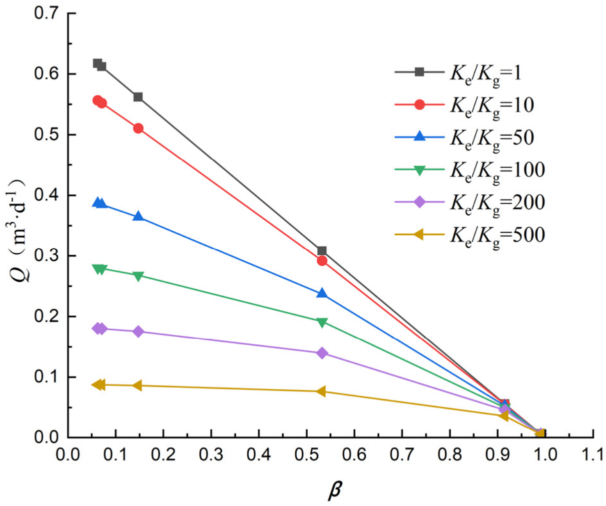

Figure 12. The relationship between Lining drainage volume and reduction coefficient.

As can be seen from Figure 12, the lining drainage and the discount factor have an inverse relationship. When the tunnel drainage is 0, i.e., the lining is impermeable and the reduction coefficient is 1. No matter how the permeability coefficient of the grouting circle is adjusted, it is impossible to change the reduction coefficient, which indicates that consideration must be given to controlling the reduction coefficient to enable the lining to have a certain degree of permeability. When $K_e/K_g \geq 100$, the discount coefficient is between 0 and 1, the trend of the discount amplitude of the tunnel drainage is slower, and the smaller the permeability coefficient of the grouting ring, the smaller the tunnel drainage. In this case, continuing to reduce the permeability coefficient of the grouting ring does not have much effect on the seepage, which shows that in the implementation of effective grouting ring plugging measures, it is necessary to ensure that the lining has a certain permeability to achieve the purpose of reducing the fold reduction coefficient. All in all, appropriately increasing the permeability coefficient of the lining and reducing the permeability coefficient of the grouting ring as much as possible are reasonable construction methods.

6. Conclusions

(1) Water pressure outside the lining will rise in response to increases in the horizontal and vertical permeability coefficients of the surrounding rock; the larger the n value, the greater the impact on external water pressure.

(2) For the H_m influenced by the K_g and t_g, a reduction in the K_g and an increase in t_g can lower the H_m. However, once the grouting circle parameter value reaches a certain

point, the effect of water plugging becomes less noticeable. Consequently, in actual projects, the parameters of the grouting layer must be judiciously managed to meet the specific requirements for tunnel water sealing.

(3) The H_m will decrease with decreasing t_m and increasing K_m, yet inadequate lining thickness may compromise tunnel construction safety. Consequently, raising the t_m and keeping a certain permeability can be an effective strategy to reduce the H_m while ensuring the structural integrity and safety of the tunnel.

(4) There is an inverse relationship between the liner drainage and the discount factor. When implementing the grouting circle to block the water, it is necessary to ensure that the lining has a certain degree of permeability, in order to better achieve the purpose of reducing the external water pressure.

(5) In addition to the above aspects, our research work still has shortcomings. The current analysis fails to fully consider the important impact of heavy rainfall infiltration on groundwater dynamics. The influence of rainfall infiltration on external water pressure should be considered in the follow-up work.

Author Contributions: Conceptualization, J.S. and Y.X.; methodology, Y.X.; software, J.S.; validation, J.S., H.M. and Y.X.; formal analysis, J.S. and H.D.; investigation, J.S. and H.M.; resources, J.S. and H.M.; data curation, J.S.; writing—original draft preparation, J.S.; writing—review and editing, Y.X.; visualization, Y.X.; supervision, H.L. and W.M.; project administration, J.S. and H.M.; funding acquisition, J.S. and H.M. All authors have read and agreed to the published version of the manuscript.

Funding: (1) Research and application of surrounding rock deformation instability mechanism and key technology of high external water pressure seepage control in Xiaolangdi north bank irrigation area engineering tunnel (Grant No. XLDBAGQ-KJGG-04). (2) The 2023 annual major scientific and technological special project in Henan Province, titled "Key Technologies for the Expansion of the Sanmenxia Reservoir Area and Systematic Management of Surrounding Small Watersheds" (231100320100).

Data Availability Statement: The data presented in this study are available in article.

Conflicts of Interest: Author Hongbin Ma was employed by the company Henan Shuitou Xiaolangdi North Bank Irrigation District Engineering Co., Ltd. The remaining authors declare that the research was conducted in the absence of any commercial or financial relationships that could be construed as a potential conflict of interest.

References

1. Hu, S.H.; Chen, Y.F.; Liu, W.; Zhou, S. Effect of seepage control on stability of a tailings dam during its staged construction with a stepwise-coupled hydro-mechanical model. *Int. J. Min. Reclam. Environ.* **2015**, *29*, 125–140. [CrossRef]
2. Dong, L.H.; Wang, H.; Song, D.Q.; Chen, J.D.; Liu, C. Analysis of the Catastrophe Mechanism and Treatment Countermeasures of a Sudden Water Inrush Disaster in a Long and Deeply Buried Tunnel in the Karst Area. *J. Perform. Constr. Fac.* **2023**, *37*, 06023002. [CrossRef]
3. Yuan, J.Q.; Chen, W.Z.; Tan, X.J.; Yang, D.S.; Wang, S.Y. Countermeasures of water and mud inrush disaster in completely weathered granite tunnels: A case study. *Environ. Earth Sci.* **2019**, *78*, 576. [CrossRef]
4. Cagri GLi, Y.D.; Yoram, R.; Li, X.J. Stochastic modeling of groundwater drawdown response induced by tunnel drainage. *Eng. Geol.* **2022**, *297*, 106529.
5. Luo, S.; Xu, M.; Kang, X.B.; Li, X.X.; Rao, L.F. Analytical solution of external water pressure on deep tunnel lining in horizontally layered hydrogeological structures. *Bull. Eng. Geol. Environ.* **2022**, *81*, 253. [CrossRef]
6. Su, K.; Yang, F.J.; Nian, F.X.; Zhu, H.Z. Anti-seepage and drainage measures of ultra-deep buried tunnel and distribution law of external water pressure of lining. *J. Cent. South Univ.* **2024**, *55*, 222–2235.
7. Ahmad, S.; Naji, M.A.; Hussain, I.; Rehman, H.; Yoo, H. Ground Saturation Response During First Filling of Lined Pressure Tunnels: A Case Study. *Rock Mech. Rock Eng.* **2020**, *54*, 513–535. [CrossRef]
8. Harr, M.E. *Groundwater and Seepage*; McGraw-Hill: New York, NY, USA, 1962; pp. 249–255.
9. Goodman, R.E.; Moye, D.G.; Schalkwyk, A.; Javandel, I. Groundwater in flows during tunnel driving. *Eng. Geol.* **1965**, *2*, 39–56.
10. Kolymbas, D.; Wagner, P. Groundwater ingress to tunnels–The exact analytical solution. *Tunn. Undergr. Space Technol.* **2006**, *22*, 23–27. [CrossRef]
11. Ying, H.W.; Zhu, C.W.; Gong, X.N. Analytic solution on seepage field of underwater tunnel considering grouting circle. *J. Zhejiang Univ.* **2016**, *50*, 1018–1023. (In Chinese)

12. Yu, J.; Zhang, Y.; Li, D.K.; Zheng, J.F.; Zhang, W.J. Analytical study of steady state seepage field in tunnels with localized water leakage under the effect of grouting circle. *Tunn. Undergr. Space Tech.* **2024**, *150*, 150105854. [CrossRef]
13. Duan, S.Q.; Jiang, X.Q.; Jiang, Q.; Xiong, J.C.; Li, C.Y. Theoretical solution and failure analysis of water pressure on lining of deep-buried non-circular hydraulic tunnel based on the equivalent hydraulic radius method. *Eng. Fail. Anal.* **2023**, *148*, 107163. [CrossRef]
14. Zhao, J.P.; Tan, Z.S.; Ma, N. Development and Application of a New Reduction Coefficient of Water Pressure on Sub-Sea Tunnel Lining. *Appl. Sci.* **2022**, *12*, 2496. [CrossRef]
15. Yu, J.; Li, D.K.; Zheng, J.F.; Zhang, Z.H.; He, Z.; Fan, Y. Analytical study on the seepage field of different drainage and pressure relief options for tunnels in high water-rich areas. *Tunn. Undergr. Space Tech.* **2023**, *134*, 105018. [CrossRef]
16. Liu, J.H.; Li, X.J. Analytical solution for estimating groundwater inflow into lined tunnels considering waterproofing and drainage systems. *Bull. Eng. Geol. Environ.* **2021**, *80*, 6827–6839. [CrossRef]
17. Bi, J.F.; Jiang, H. Water infiltration in drained circular tunnels: An analytical solution and its simplification. *Géotechnique* **2023**, *in press*. [CrossRef]
18. Wang, X.R.; Liu, X.F.; Wang, E.Y.; Liu, S.X.; Shan, T.C. Microcracking Characterization in Tensile Failure of Hard Coal: An Experimental and Numerical Approach. *Rock Mech. Rock Eng.* **2024**, *57*, 6441–6460. [CrossRef]
19. Hassani, N.A.; Farhadian, H.; Katibeh, H. A comparative study on evaluation of steady-state groundwater inflow into a circular shallow tunnel. *Tunn. Undergr. Space Tech.* **2018**, *73*, 15–25. [CrossRef]
20. Arjnoi, P.; Jeong, J.H.; Kim, C.Y.; Park, K.H. Effect of drainage conditions on porewater pressure distributions and lining stresses in drained tunnels. *Tunn. Undergr. Space Tech.* **2009**, *24*, 376–389. [CrossRef]
21. Zhang, Z.J.; Zeng, C.P.; Li, H.; Gao, Y.; Guo, L.; Li, Y.X.; Liang, H.F.; Zhang, E.Z. Optimal Design of the Seepage Control for Xianglushan Diversion Tunnel Under High External Water Pressure. *Geotech. Geol. Eng.* **2022**, *40*, 4595–4615. [CrossRef]
22. Yu, B.X.; Chen, Z.Q.; Li, Z.; Chen, K.P.; Zhang, H.; He, C. Analysis of water pressure distribution and optimization of waterproof-drainage system for tunnels in water-rich region. *Bull. Eng. Geol. Environ.* **2024**, *83*, 137. [CrossRef]
23. Li, P.F.; Liu, H.C.; Zhao, Y.; Li, Z. A bottom-to-up drainage and water pressure reduction system for railway tunnels. *Tunn. Undergr. Space Tech.* **2018**, *81*, 296–305. [CrossRef]
24. Lv, Y.X.; Jiang, J.; Chen, L.; Hu, W.; Jiang, Y.J. Elaborate simulation and predication of the tunnel drainage effect on karst groundwater field and discharge based on Visual MODFLOW. *J. Hydrol.* **2022**, *612*, 128023. [CrossRef]
25. Park, K.; Owatsiriwong, A.; Lee, J. Analytical solution for steady-state groundwater inflow into a drained circular tunnel in a semi-infinite aquifer: A revisit. *Tunn. Undergr. Space Technol.* **2007**, *23*, 206–209. [CrossRef]
26. Zhang, J.W.; Zeng, X.T.; Tan, Y. Analytical solution for deep pressure tunnels using composite stratum under a groundwater table. *Ain Shams Eng. J.* **2020**, *12*, 1419–1434.
27. Li, L.; Chen, H.H.; Li, J.P.; Sun, D. A semi-analytical solution to steady-state groundwater inflow into a circular tunnel considering anisotropic permeability. *Tunn. Undergr. Space Tech.* **2021**, *116*, 104115. [CrossRef]
28. Yan, Q.X.; Zhang, T.; Zhang, C.; Guo, D.P.; Qing, S.Y. Analytical solution for steady seepage into a circular deep-buried mountain tunnel with grouted zone in anisotropic strata. *J. Mt. Sci.* **2022**, *19*, 2987–2998. [CrossRef]